

Article

Factors to Enable Crystallization of Environmentally Stable Bioscorodite from Dilute As(III)-Contaminated Waters

Masahito Tanaka and Naoko Okibe *

Department of Earth Resources Engineering, Faculty of Engineering, Kyushu University, 744 Motoooka, Nishi-ku, Fukuoka 819-0395, Japan; m-tanaka13@mine.kyushu-u.ac.jp

* Correspondence: okibe@mine.kyushu-u.ac.jp; Tel.: +81-92-802-3312

Received: 22 December 2017; Accepted: 12 January 2018; Published: 15 January 2018

Abstract: Applicability of the bioscorodite method (use of the thermo-acidophilic Fe(II)-oxidizing archaeon *Acidianus brierleyi* for arsenic (As) oxidation and immobilization at 70 °C) was tested for synthetic copper refinery wastewaters of a wide range of dilute initial As(III) concentrations ($[\text{As(III)}]_{\text{ini}} = 3.3\text{--}20$ mM) with varying initial $[\text{Fe(II)}]/[\text{As(III)}]$ molar ratios ($[\text{Fe(II)}]_{\text{ini}}/[\text{As(III)}]_{\text{ini}} = 0.8\text{--}6.0$). Crystallization of scorodite ($\text{FeAsO}_4 \cdot 2\text{H}_2\text{O}$) tends to become increasingly challenging at more dilute As(III) solutions. Optimization of conditions such as initial pH, seed feeding and initial $[\text{Fe(II)}]/[\text{As(III)}]$ molar ratio was found critical in improving final As removal and product stability: Whilst setting the initial pH at 1.2 resulted in an immediate single-stage precipitation of crystalline bioscorodite, the initial pH 1.5 led to a two-stage As precipitation (generation of brown amorphous precursors followed by whitish crystalline bioscorodite particles) with a greater final As removal. The formation process of bioscorodite precipitates differed significantly depending on the type of seed crystals fed (bio- versus chemical- scorodite seeds). Feeding the former was found effective not only in accelerating the reaction, but also in forming more recalcitrant bioscorodite products (0.59 mg/L; Toxicity Characteristic Leaching Procedure (TCLP) test). Under such favorable conditions, 94–99% of As was successfully removed as crystalline bioscorodite at all dilute As(III) concentrations tested by setting $[\text{Fe(II)}]_{\text{ini}}/[\text{As(III)}]_{\text{ini}}$ at 1.4–2.0. Providing an excess Fe(II) (closer to $[\text{Fe(II)}]_{\text{ini}}/[\text{As(III)}]_{\text{ini}} = 2.0$) was found beneficial to improve the final As removal (up to 98–99%) especially from more dilute As(III) solutions.

Keywords: *Acidianus brierleyi*; thermo-acidophilic archaeon; arsenic; scorodite; As(III) and Fe(II) oxidation

1. Introduction

Arsenic (As) contamination is a growing problem in metallurgical operations due to the increasing metal demand that necessitates processing of As-bearing low-grade copper sulfide ores such as enargite (Cu_3AsS_4) and tennantite ($\text{Cu}_{12}\text{As}_4\text{S}_{13}$). As one of the approaches to immobilize soluble As species from wastewaters, formation of scorodite ($\text{Fe}^{\text{III}}\text{As}^{\text{V}}\text{O}_4 \cdot 2\text{H}_2\text{O}$) is considered an ideal form of As disposal due to its high thermodynamic stability, low iron demand and high density [1]. Early studies on scorodite synthesis employed hydrothermal processes targeting high As(V) concentrations of 170–460 mM (13,000–35,000 mg/L) [2,3]. They were later followed by studies using atmospheric pressure (mostly at around 95 °C), again targeting high As(V) concentration ranges of 130–670 mM (10,000–50,000 mg/L) [4–10]. While these chemical approaches are generally effective for high As(V) concentrations, even after treatments with a good As removal efficiency, residual soluble As(V) must yet meet the effluent standard (e.g., 95% As removal from $[\text{As(V)}]_{\text{ini}} = 10,000$ mg/L would still leave 500 mg/L of residual As(V) in solution [7]). Also, since such chemical treatments generally require a

pretreatment step to oxidize As(III) to less toxic and less mobile As(V) using strong chemical oxidants prior to the scorodite precipitation step, residual As(III) can still persist in the solutions. There are also cases where dilute As(III) solutions (up to 25 mM) are produced in metallurgical operations, such as from solid-liquid separation followed by Cu recovery after enargite concentrate leaching, wherein chemical scorodite synthesis turns ineffective (JX Nippon Mining & Metals Co., Ltd., Tokyo, Japan; personal communication).

Hence, to realize effective scorodite formation even from dilute As solutions, a microbiological approach using Fe(II)-oxidizing thermophiles (72–80 °C) was proposed by Gonzalez-Contreras et al. (2010, 2012a, 2012b) using 13–37 mM (1000–2800 mg/L) As(V) as starting reactant [11–13]. Later our studies enabled simultaneous microbial As(III) and Fe(II) oxidation using the thermophilic archaeon *Acidianus brierleyi* (70 °C), which for the first time realized one-step bioscorodite crystallization from original wastewater solutes of As(III) and Fe(II), without necessitating any As(III) oxidation pretreatments or chemical oxidants [14,15]: So far bioscorodite was successfully produced by *Ac. brierleyi* from 13 mM (1000 mg/L) of As(III) directly, with 86–99% final As removal depending on initial conditions [14]. Whilst scorodite crystallization becomes more difficult at more dilute As concentrations under milder temperature condition, exploiting factors to enable such reaction is of great importance to broaden the applicability of the scorodite method for a wide range of As(III)-contaminated waters.

From studies of conventional abiotic scorodite syntheses, seed feeding (scorodite or other heterogeneous crystals) was shown to be one of the influential factors to promote scorodite formation [4,6,16]. Initial pH was also reported to affect the stability and Fe/(As + S) ratio of the resultant scorodite product [17]. Initial solution Fe/As ratio is also an affecting factor; in hydrothermal scorodite synthesis at 150 °C, the rate of As precipitation decreased with increasing initial solution Fe(III)/As(V) molar ratios from 1.0 to 1.5 and 2.0 [3]. Our previous bioscorodite study also found that the form of As precipitation changes at different initial solution Fe(II)/As(III) ratios [14].

Based on the above, the aim of this study was set to find factors that enable effective bioscorodite crystallization from dilute As(III)-bearing solutions (3.3–6.5 mM; so far undescribed by scorodite studies): In particular, (i) bio- and chemical- scorodite particles were produced to compare their characteristics; (ii) their effectiveness as seed crystals was evaluated for the bioscorodite crystallization reaction from dilute 4.7 mM As(III) solution (wherein initial pHs 1.5 or 1.2 also compared); (iii) stability of the resultant bioscorodite products was evaluated by the toxicity characteristic leaching procedure (TCLP) test, and finally; (iv) a range of As(III) solutions (3.3–20 mM) with varying initial [Fe(II)]/[As(III)] molar ratios (0.8–6.0) was tested for bioscorodite crystallization to grasp the overall applicability of the bioscorodite method.

2. Materials and Methods

2.1. Microorganism

Acidianus brierleyi DSM 1651^T was maintained and pre-grown in 200 mL heterotrophic basal salts (HBS) medium (450 mg/L (NH₄)₂SO₄; 50 mg/L KCl, 50 mg/L KH₂PO₄; 500 mg/L MgSO₄·7H₂O; 14 mg/L Ca(NO₃)₂·4H₂O; 142 mg/L Na₂SO₄; pH 1.5 with H₂SO₄) [18] in 500 mL Erlenmeyer flasks containing 18 mM Fe(II) (1000 mg/L; as FeSO₄·7H₂O), 13 mM As(III) (1000 mg/L; as NaAsO₂), and 0.02% (*w/v*) yeast extract. Flasks were incubated at 70 °C, shaken at 100 rpm.

2.2. Preparation of Bio- and Chemical- Scorodite As Seed Crystals

Bioscorodite seeds: *Ac. brierleyi* was grown as described in Section 2.1 for 14 days.

Chemical scorodite seeds: Five-hundred milliliter Erlenmeyer flasks containing 200 mL deionized water (pH 1.5 with H₂SO₄) with 358 mM Fe(II) (20 g/L; as FeSO₄·7H₂O) and 267 mM As(V) (20 g/L; as Na₂HAsO₄·7H₂O) were incubated at 70 °C, shaken at 100 rpm for 7 days.

The resultant bio- and chemical- scorodite particles were collected respectively and freeze-dried overnight. Production of seed crystals did not involve seed feeding.

2.3. Bioscorodite Crystallization Experiment

Ac. brierleyi was pre-grown and inoculated into 200 mL HBS medium (pH 1.5 or 1.2 with H₂SO₄; 500 mL flasks) containing 3.3–20 mM As(III), 4.5–28 mM Fe(II) ([Fe(II)]_{ini}/[As(III)]_{ini} molar ratio = 0.8–6.0) and 0.02% yeast extract. The initial cell density was set to 1.0 × 10⁷ cells/mL. Bio- or chemical-scorodite seeds were fed at 0.15% (*w/v*) where indicated. Flasks were incubated at 70 °C, shaken at 100 rpm. Samples were regularly withdrawn to monitor pH, Eh (vs. SHE), cell density (Thoma counting chamber) and concentrations of Fe(II) (*O*-phenanthroline method), As(III) (stripping voltammetric method; Nano-band explorer, GL Sciences, Tokyo, Japan) and total soluble Fe and As (ICP-OES; Optima8300, PerkinElmer, Waltham, MA, USA). All experiments were conducted in duplicates.

2.4. Toxicity Characteristic Leaching Procedure (TCLP) Test

The TCLP test was conducted by following the EPA method 1311 [19]. Original scorodite seeds formed in Section 2.2 and final bioscorodite products formed in Section 2.3 (at [As(III)]_{ini} = 4.7 mM; [Fe(II)]_{ini} = 9.5 mM) were transferred into 25 mL vials containing 10 mL acetate buffer (pH 4.9) at a pulp density of 5% (*w/v*) and incubated at 25 °C, rotated at 30 rpm for 18 h. Liquid samples were filtered (0.45 μm glass fiber) to measure total soluble Fe and As concentrations. Tests were conducted in duplicates.

2.5. Ion Activity Product (IAP) Calculation

The IAP of bioscorodite was calculated as Equation (1), based on its congruent dissolution (Equation (2)). Ionic activities of Fe(III) and As(V) were calculated from Equations (3) and (4), using the measured pH values ($a_{\text{H}^+} = 10^{-\text{pH}}$) and total soluble concentrations of Fe(III) and As(V) (M), respectively. The hydrolysis constants (K_i) at 70 °C were calculated using the van't Hoff equation (Equation (5), Table A1) [11,20].

$$\text{IAP}_{\text{scorodite}} = (a_{\text{Fe}^{3+}})(a_{\text{AsO}_4^{3-}}) \quad (1)$$



$$a_{\text{Fe}^{3+}} = \frac{\text{Fe(III)}_{\text{total}}}{1 + \frac{K_{\text{Fe1}}}{a_{\text{H}^+}} + \frac{K_{\text{Fe1}}K_{\text{Fe2}}}{(a_{\text{H}^+})^2} + \frac{K_{\text{Fe1}}K_{\text{Fe2}}K_{\text{Fe3}}}{(a_{\text{H}^+})^3} + \frac{K_{\text{Fe1}}K_{\text{Fe2}}K_{\text{Fe3}}K_{\text{Fe4}}}{(a_{\text{H}^+})^4}} \quad (3)$$

$$a_{\text{AsO}_4^{3-}} = \frac{\text{As(V)}_{\text{total}}}{1 + \frac{a_{\text{H}^+}}{K_{\text{As3}}} + \frac{(a_{\text{H}^+})^2}{K_{\text{As2}}K_{\text{As3}}} + \frac{(a_{\text{H}^+})^3}{K_{\text{As1}}K_{\text{As2}}K_{\text{As3}}}} \quad (4)$$

$$-\ln K_{70\text{ }^\circ\text{C}} = -\ln K_{25\text{ }^\circ\text{C}} + \frac{\Delta H_r^0}{R} \left(\frac{1}{T_{70\text{ }^\circ\text{C}}} - \frac{1}{T_{25\text{ }^\circ\text{C}}} \right) \quad (5)$$

where ΔH_r^0 , standard reaction enthalpy (kJ/mol); T , temperature (K); R , gas constant = 8.314 (J/mol·K).

2.6. Solid Analysis

Precipitates were collected at designated times by filtration and freeze-dried overnight for X-ray diffraction (XRD; Ultima IV, Rigaku, Tokyo, Japan; Cu K α 40 mA, 40 kV), Fourier transform infrared spectroscopy (FT/IR-670Plus, JASCO, Tokyo, Japan; KBr pellet method), thermo gravimetry (TG-DTA2000SA, Bruker AXS, Karlsruhe, Germany; by heating from room temperature to 500 °C at 10 °C/min at 100 mL/min N₂) and scanning electron microscope (SEM; ULTRA55, ZEISS, Oberkochen, Germany) analyses. Precipitates were embedded in an epoxy resin (SpeciFix-20, Struers, Ballerup, Denmark), polished using 2000 and 4000 grit emery papers on a polishing machine (Doctor Lap

ML-182, Maruto, Tokyo, Japan) and carbon-sputtered (JEC-560, JEOL, Tokyo, Japan) to observe SEM cross-section views. The scorodite particle size was measured using a laser diffraction particle size distribution analyzer (Partica LA-950, HORIBA, Kyoto, Japan). Following the drying pre-treatment at 80 °C for 50 h, BET specific surface area measurements were performed on scorodite seeds (BEL-Max, MicrotracBEL, Osaka, Japan). To analyze the chemical composition of original seed crystals and final bioscorodite products, 50 mg of dried sample was digested in 10 mL of 35% HCl and concentrations of soluble Fe and As were measured by ICP-OES.

3. Results and Discussion

3.1. Effect of Seed Feeding and pH

3.1.1. Characterization of Scorodite Seeds

Scorodite seed crystals were prepared by either biological or chemical methods and identified by XRD (Figure 1a). According to TG-DTA analysis, weight losses (at 125–250 °C) of bioscorodite and chemical scorodite seeds were 12.5% and 15.0%, respectively (Figure 1b), suggesting that their structural water contents were $\text{FeAsO}_4 \cdot 1.55\text{H}_2\text{O}$ and $\text{FeAsO}_4 \cdot 1.91\text{H}_2\text{O}$, respectively (cf. the theoretical structural water content is 15.6% for scorodite ($\text{FeAsO}_4 \cdot 2\text{H}_2\text{O}$)). A gradual and continuous weight loss observed with bioscorodite (but not with chemical scorodite) was likely from the result of decomposition of organic matters deriving from cells, as was detected by FT-IR (Figure 1c). Different XRD peak sharpness between bio- and chemical- scorodite seeds (Figure 1a) may, therefore, reflect difference in their crystallinity due to encrustation of cells within bioscorodite particles (Figure 1c) as well as in their structural water content (Figure 1b).

Morphological differences were clearly seen by SEM observation. Chemical scorodite seeds were aggregates of orthorhombic crystals (Figure 2d,e), with the average particle size and specific surface area of 98 μm and 0.7 m^2/g , respectively (Table 1). Meanwhile, bioscorodite seeds were found as spherical aggregates (Figure 2a,b) with the average particle size and specific surface area of 36 μm and 2.0 m^2/g , respectively (Table 1). There was a significant difference in crystal surface roughness and small almond-shaped grains covered the bioscorodite surface (Figure 2b). SEM cross-section views found hollow bioscorodite particles (Figure 2c) whereas chemical scorodite particles were completely filled (Figure 2f). Other than the presence/absence of cells, this morphology difference may be partly attributed to Fe and As ionic species available during the scorodite crystallization process: In the chemical process, As(V) is initially fed where Fe(III) is gradually provided from Fe(II) oxidation by dissolved oxygen. In the biological process, on the other hand, microbial Fe(II) oxidation to Fe(III) is rapidly completed, after which As(V) is gradually provided by microbial As(III) oxidation.

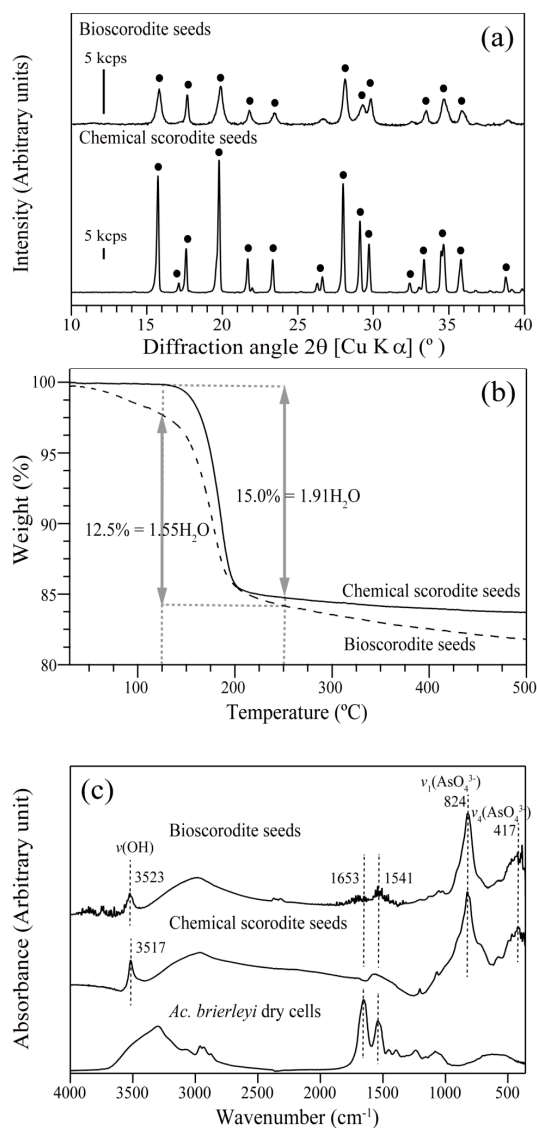


Figure 1. Characterization of bioscorodite and chemical scorodite by XRD (a), TG-DTA (b) and FT-IR (c) analyses. (a) The symbol ● is assigned to scorodite (JCPDS 37-0468). (b) The structural water content was calculated based on the weight loss at 125–250 °C of bioscorodite (broken line) and chemical scorodite (solid line). (c) Dotted lines at 417 and 824 cm^{-1} can be assigned to AsO_4^{3-} stretching vibration (436 and 825 cm^{-1}) [21] and those at 3523 and 3517 cm^{-1} to OH stretching vibration (3511 cm^{-1}) [22]. Two peaks at 1541 and 1653 cm^{-1} are attributed to cell proteins (1545 and 1654 cm^{-1}) [23].

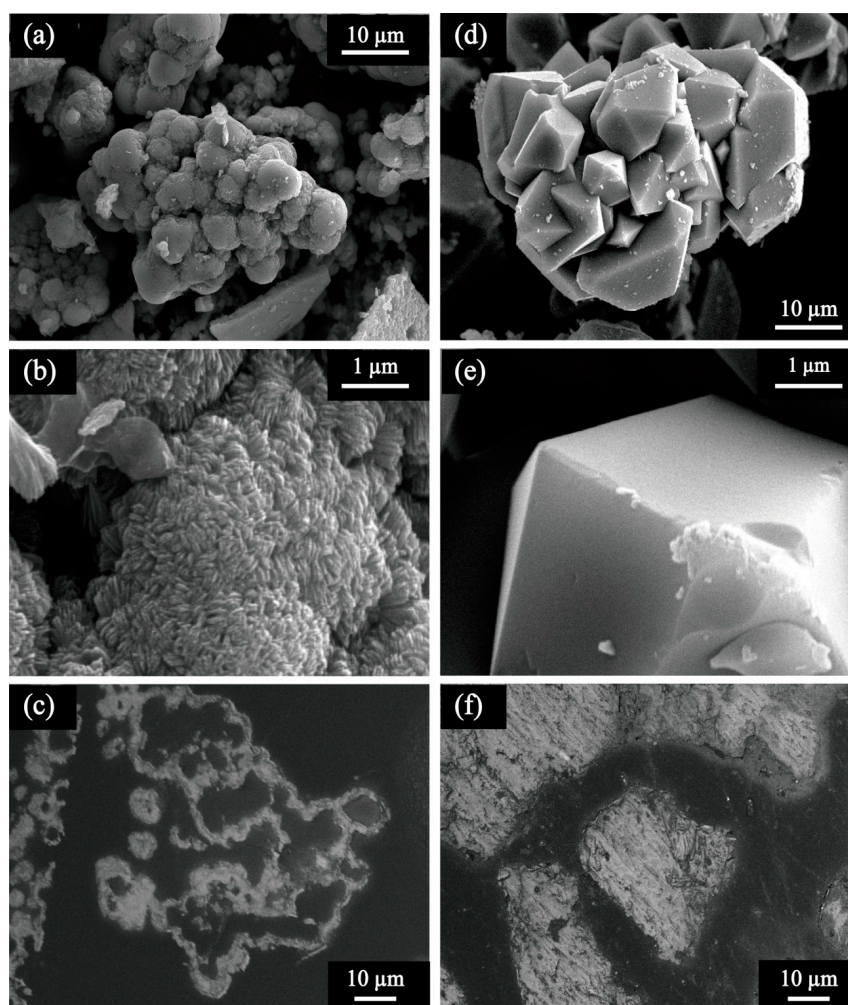


Figure 2. SEM images of (a–c) bio- and (d–f) chemical- scorodite seed crystals at 2000× (a,d) or 20,000× (b,e) magnification. Cross-section views are shown at 3000× magnification (c,f).

Table 1. Particle size and specific surface area of bio- and chemical- scorodite seed crystals.

Seed Crystal	Particle Size (μm)			Specific Surface Area (m ² /g)
	Average	Median	Mode	
Bioscorodite Seeds	36	35	36	2.0
Chemical Scorodite Seeds	98	91	90	0.7

3.1.2. Effect of Seed Feeding

Seeding effects of bio- and chemical- scorodite particles were compared at $[\text{As(III)}]_{\text{ini}} = 4.7 \text{ mM}$, $[\text{Fe(II)}]_{\text{ini}} = 9.5 \text{ mM}$, and pH 1.5.

Although the microbial oxidation speed of As(III) and Fe(II) was not affected in all cases, a clear difference in As and Fe precipitation behaviors was found at pH 1.5 (Figure 3a,b). The first-stage As removal observed at day 0–2 (brown-colored amorphous precursor formation [15]) was an almost common phenomenon, but the second-stage As removal observed at day 14–21 (whitish green-colored scorodite formation [15]) was promoted on bioscorodite seeds only, resulting in 98% As removal at day 21 (Figure 3a,b).

The supersaturation of scorodite was evaluated based on the ion activity product (IAP) (Figure 3c) calculated from Fe(III) and As(V) ion activities (Figure 3d,e). The $\log K_{\text{sp}}$ for scorodite was reported to be -25.8 [24]. The greater first-stage As-removal on bioscorodite seeds (than on chemical scorodite

seeds; Figure 3a) led to the lower and stable supersaturation level during day 2–14 (Figure 3c), before a sudden second-stage As removal was triggered to produce crystalline scorodite (Figure 3a).

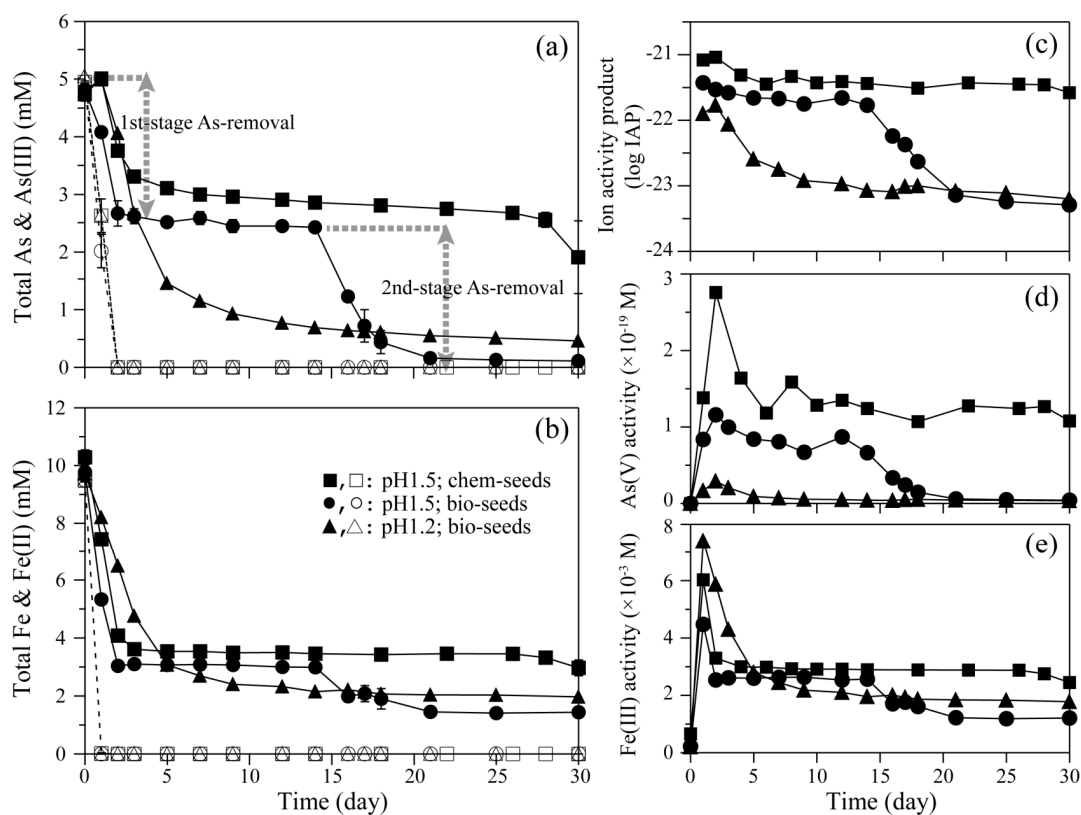


Figure 3. Bioscorodite crystallization test by feeding different seed crystals at pH 1.5 or pH 1.2: Bio- (pH 1.5; ● ○/pH 1.2; ▲ △) or chemical- (pH 1.5; ■ □) scorodite seeds were fed at 0.15%. $[\text{As(III)}]_{\text{ini}} = 4.7$ mM. $[\text{Fe(II)}]_{\text{ini}} = 9.5$ mM. (a) Concentrations of total soluble As (solid lines and filled symbols) and As(III) (broken lines and open symbols). Dotted arrows indicate the first- (day 0–2) and second-stage (day 14–21) As-removal on bioscorodite seeds at pH 1.5. (b) Concentrations of total soluble Fe (solid lines and filled symbols) and Fe(II) (broken lines and open symbols). (c) Ion activity product of bioscorodite. (d) As(V) ion activity. (e) Fe(III) ion activity.

SEM cross section views revealed contrasting bioscorodite crystallization patterns on bio- (Figure 4(a1–a6)) and chemical- scorodite seeds (Figure 4b). Hollow bioscorodite seed particles were found increasingly filled with newly formed scorodite (Figure 4(a1–a6)), whilst solid chemical seeds induced their surface to be thoroughly coated with new scorodite precipitates (Figure 4(b1–b6)).

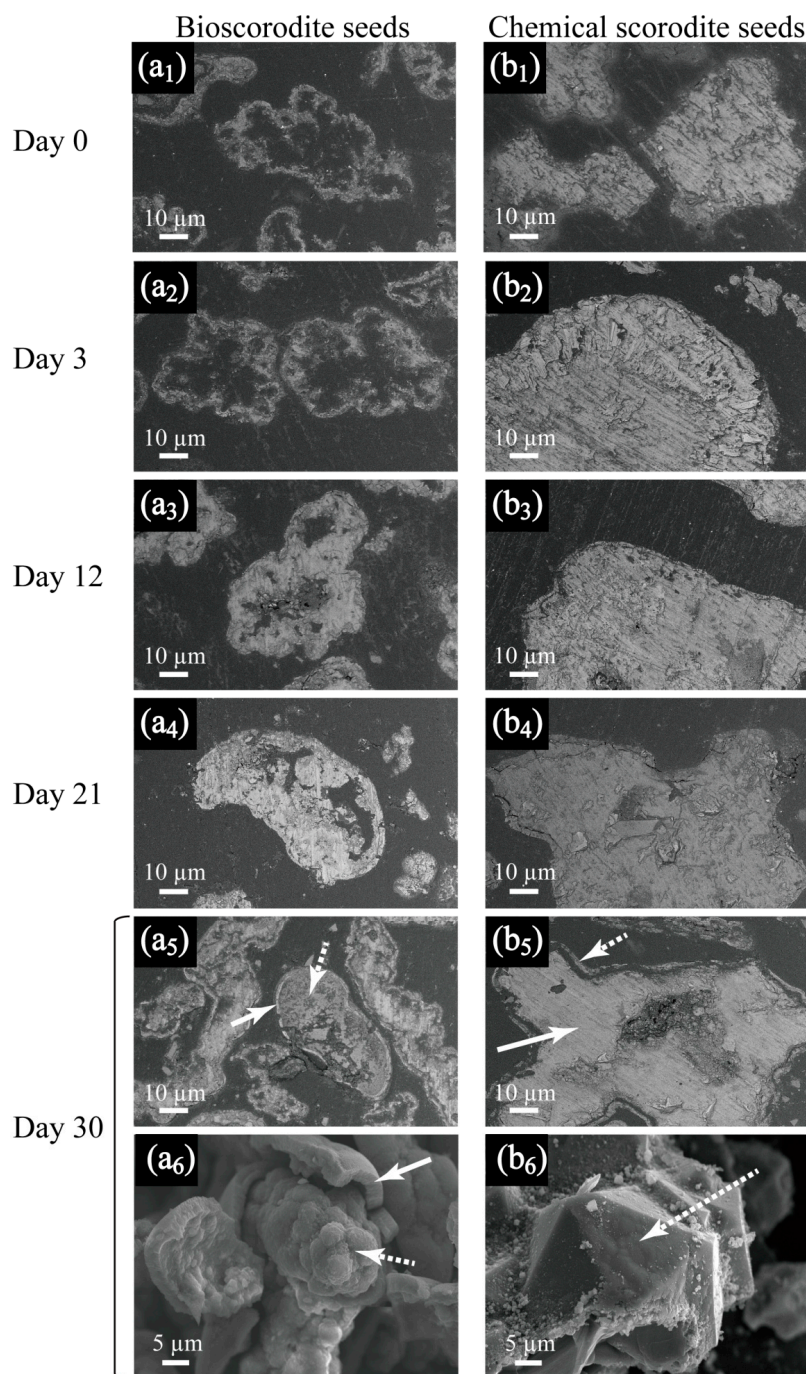


Figure 4. SEM cross section images depicting bioscorodite crystallization process (from day 0 to day 30) on bio- (from **a1** to **a5**) or chemical- scorodite seeds (from **b1** to **b5**), respectively. SEM whole view images of the resultant particles (day 30) on bio- (**a6**) or chemical- scorodite seeds (**b6**) are also shown. Solid and dotted arrows (**a5,a6,b5,b6**) indicate locations of seed crystals and fresh scorodite precipitates, respectively.

Other abiotic studies under atmospheric pressure condition using As(V) and Fe(III) as starting species also have reported a positive effect of seeds with high specific surface area, e.g., the better scorodite precipitation kinetics were observed by using finer seeds such as hematite and hydrothermal scorodite [6]. Caetano et al. (2009) reported that a specific surface area higher than 270 m²/g was required to achieve 85% As removal [16].

The fact that the specific surface area of bioscorodite ($2.0 \text{ m}^2/\text{g}$; Table 1) was nearly three-times greater than that of chemical scorodite ($0.7 \text{ m}^2/\text{g}$; Table 1) likely allowed the former to show better seeding effect.

3.1.3. Effect of Initial pH

Effect of initial pH values (1.5 and 1.2) on bioscorodite crystallization was studied at $[\text{As(III)}]_{\text{ini}} = 4.7 \text{ mM}$, $[\text{Fe(II)}]_{\text{ini}} = 9.5 \text{ mM}$ using bioscorodite seeds.

Chemical scorodite syntheses are generally conducted at pH 1.0 or lower [2,6,8,9,25]. Fujita et al. (2009) chemically synthesized stable scorodite particles at the pH range of 0.3–1.0, but higher pH levels (pH > 1.2) negatively affected scorodite stability [17]. Therefore, the effect of lowering pH was also tested here. Although As(III) and Fe(II) oxidation tendencies by *Ac. brierleyi* were not affected, lowering pH from 1.5 to 1.2 (using bioscorodite seeds) resulted in a different As removal behavior: A continuous formation of whitish bioscorodite particles was observed from the beginning at pH 1.2, instead of displaying two-stage As removal at pH 1.5 (Figure 3a). However, As removal remained relatively incomplete at pH 1.2 (91%), compared to at pH 1.5 (98%) (at day 30; Figure 3a). Overall lower supersaturation levels (Figure 3c) owing to lower As(V) ion activities at pH 1.2 (Figure 3d) as well as continuous As precipitation likely promoted steady and continuous bioscorodite crystal growth, as was reported under abiotic atmospheric pressure conditions [4,5,16].

3.1.4. Stability of Final Bioscorodite Products

TCLP tests were conducted for original scorodite seeds (bio- and chemical seeds) as well as for the resultant bioscorodite products (Table 2).

Original seed crystals: Despite their smaller particle size and larger specific surface area (Table 1), bioscorodite seeds showed greater stability (As; $0.33 \pm 0.08 \text{ mg/L}$; Table 2) compared to chemical scorodite seeds (As; $5.49 \pm 0.03 \text{ mg/L}$; Table 2). Although the Fe/As molar ratios of all scorodite seeds and products were 1.0–1.1 and 1.3–1.4, respectively, the amount of Fe leached generally remained only below one-tenth of that of As (Table 2), due to selective re-precipitation of Fe(III) at pH 4.9. Other chemical scorodite studies reported TCLP leachabilities ranging 0.1–13.6 As-mg/L [7,10,16], generally often higher than those of bioscorodite (Table A2). Such stability difference between bioscorodite seeds and chemical seeds may be attributed to factors such as involvement of cell encrustation, structural water content and morphological difference, and crystal maturity (speed of crystallization), but the exact reasons remain to be unclear.

Final bioscorodite products: Stability of final bioscorodite products was improved (As; from 5.49 ± 0.03 to $1.86 \pm 0.05 \text{ mg/L}$; Table 2) when chemical seed surface became coated with fresh bioscorodite precipitates, whilst As leachability remained at a low level both before (As; $0.33 \pm 0.08 \text{ mg/L}$) and after (As; $0.59 \pm 0.08 \text{ mg/L}$) the bioscorodite crystallization reaction when biological seeds were used (Table 2). Lowering initial pH to 1.2 using bioscorodite seeds slightly improved the product stability (As; $0.20 \pm 0.01 \text{ mg/L}$), compared to that at pH 1.5 (As; $0.59 \pm 0.20 \text{ mg/L}$; Table 2), although the final As removal was lower at pH 1.2 (Figure 3a).

Table 2. TCLP test results for original scorodite seed crystals (bio- and chemical-) and final bioscorodite products.

Conditions Used for Bioscorodite Crystallization Reaction		Original Seed Crystals ^a					Final Bioscorodite Products ^b				
		TCLP Leachability		Chemical Composition (Weight in 50 mg Sample; mg)			TCLP Leachability		Chemical Composition (Weight in 50 mg Sample; mg)		
Seed Crystals Fed	Initial pH	[As] (mg/L)	[Fe] (mg/L)	Fe	As	Fe/As Molar Ratio	[As] (mg/L)	[Fe] (mg/L)	Fe	As	Fe/As Molar Ratio
Bioscorodite	1.5	0.33 ± 0.08	<0.004	11.7	14.1	1.1	0.59 ± 0.20	<0.004	12.1	12.0	1.4
	1.2			(0.21 mmol)	(0.19 mmol)		0.20 ± 0.01	0.11 ± 0.03	(0.21 mmol)	(0.16 mmol)	1.3
Chemical scorodite	1.5	5.49 ± 0.03	0.11 ± 0.01	9.12	12.2	1.0	1.86 ± 0.05	0.005	10.5	11.2	1.3
				(0.16 mmol)	(0.16 mmol)				(0.19 mmol)	(0.15 mmol)	

^a Bioscorodite seeds were produced at [As(III)]_{ini} = 13 mM and [Fe(II)]_{ini} = 18 mM (Fe(II)/As(III) = 1.4), whereas chemical scorodite seeds at [As(V)]_{ini} = 267 mM and [Fe(II)]_{ini} = 358 mM (Fe(II)/As(V) = 1.3). ^b Final bioscorodite products were produced at [As(III)]_{ini} = 4.7 mM and [Fe(II)]_{ini} = 9.5 mM (Fe(II)/As(III) = 2.0) using either bio- or chemical scorodite seeds.

Overall, by comparing results at pH 1.5, it can be said that the use of bioscorodite seeds is advantageous from the following viewpoints; (i) significantly improved final As removal (Figure 3a) (at least partly due to their larger specific surface area; Table 1); (ii) higher product stability (lower TCLP leachability of As); and (iii) hollows of bioscorodite particles can be filled by fresh precipitates.

3.2. Optimal Fe(II)/As(III) Molar Ratios for As Removal as Bioscorodite from a Range of Dilute As(III)-Bearing Solutions

Following the above findings that feeding bioscorodite seeds and setting initial pH to 1.5 have favorable effects to improve bioscorodite formation from dilute As(III) solution (4.7 mM), a range of initial As(III) concentrations (3.3–20 mM) were tested to find their respective optimal Fe(II)/As(III) molar ratio under these conditions. Feeding (even at 0.15%) of bioscorodite seeds was found significantly effective especially when targeting more dilute $[\text{As(III)}]_{\text{ini}}$ of 3.3 mM (95% or 11% As removal with or without seeds, respectively at $[\text{Fe(II)}]_{\text{ini}}/[\text{As(III)}]_{\text{ini}} = 1.4$; Table 3), and of 4.7 mM (94% or 15% As removal with or without seeds, respectively at $[\text{Fe(II)}]_{\text{ini}}/[\text{As(III)}]_{\text{ini}} = 1.4$; Table 3). The optimal $[\text{Fe(II)}]_{\text{ini}}/[\text{As(III)}]_{\text{ini}}$ ratio was generally 1.4–2.0 at all $[\text{As(III)}]_{\text{ini}}$ tested, enabling 94–99% As removal as scorodite (although starting at lower $[\text{As(III)}]_{\text{ini}}$ required longer incubation time), of which, providing an excess Fe(II) (closer to $[\text{Fe(II)}]_{\text{ini}}/[\text{As(III)}]_{\text{ini}} = 2.0$) was found beneficial to improve the final As removal (up to 98–99%) especially from more dilute As(III) solutions (Table 3). Setting $[\text{Fe(II)}]_{\text{ini}}/[\text{As(III)}]_{\text{ini}} = 1.0$ (theoretical Fe/As molar ratio of scorodite) produced scorodite but with a decreased final As removal. On the other hand, setting $[\text{Fe(II)}]_{\text{ini}}/[\text{As(III)}]_{\text{ini}} \geq 2.5$ –3.0 led to formation of unwanted amorphous precipitates or jarosite at all initial As(III) concentrations tested (Table 3). In abiotic hydrothermal/atmospheric pressure methods starting with high concentrations of oxidized species, the presence of excess Fe(III) (e.g., $[\text{Fe(III)}]_{\text{ini}}/[\text{As(V)}]_{\text{ini}} > 1.5$) generally negatively affected the precipitation kinetics of scorodite and, thus, the ratios of 1.0–1.5 are used [3,7,25]. However, when treating these dilute, reduced species of As(III) and Fe(II) as starting materials microbiologically, it was found that Fe(III) should be added to an slight excess of $1.4 \leq [\text{Fe(III)}]_{\text{ini}}/[\text{As(V)}]_{\text{ini}} \leq 2.0$ for the best performance. Chemical composition of the resultant bioscorodite products ($[\text{Fe}]_{\text{im}}/[\text{As}]_{\text{im}}$ ratio) generally became closer to 1.0 (the theoretical ratio for scorodite) at higher initial As(III) concentrations (Table 3). Slightly higher $[\text{Fe}]_{\text{im}}/[\text{As}]_{\text{im}}$ ratios (1.2–1.5) observed at lower initial As(III) concentrations may be due to incorporation of SO_4^{2-} , as was reported in abiotic hydrothermal [25–28] and atmospheric scorodite synthesis [7].

Table 3. Evaluation of $[\text{As(III)}]_{\text{ini}}$ and $[\text{Fe(II)}]_{\text{ini}}/[\text{As(III)}]_{\text{ini}}$ molar ratios for final As removal as bioscorodite (pH 1.5; with or without bioscorodite seed feeding).

Initial Media Condition			Seed Feeding (Bioscorodite; %)	Final As Removal		Solid Analysis	Secondary Mineral Identified	References
$[\text{As(III)}]_{\text{ini}}$ (mM)	$[\text{Fe(II)}]_{\text{ini}}$ (mM)	$[\text{Fe(II)}]_{\text{ini}}/[\text{As(III)}]_{\text{ini}}$ Molar Ratio		(%)	(Days)	$[\text{Fe}]_{\text{im}}/[\text{As}]_{\text{im}}$ Molar Ratio		
3.3 (250 ppm)	4.5	1.4	0	11	24	-	Amorphous	This study
				95		1.2	Scorodite	
	6.5 13.5 20.0	2.0 4.0 6.0	0.15	98		1.2	Scorodite	
				59		-	Jarosite	
				59		-	Jarosite	
4.7 (350 ppm)	6.3	1.4	0	15	21	-	Amorphous	This study
				80		-	Scorodite	
	4.7 6.5 9.5 14.0 19.0	1.0 1.4 2.0 3.0 4.0	0.15	94		1.5	Scorodite	
				98		1.4	Scorodite	
				53		-	Amorphous	
				65		-	Jarosite	
6.5 (500 ppm)	6.5	1.0		84	20	1.1	Scorodite	This study
				97		1.1	Scorodite	
	9.0 10.5 12.0 13.0 16.5 19.5	1.4 1.6 1.8 2.0 2.5 3.0	0.15	98		1.1	Scorodite	
				99		1.1	Scorodite	
				99		1.1	Scorodite	
				71		-	Amorphous	
				71		-	Jarosite	
13.0 (1000 ppm)	18.0	1.4	0	99	14	1.1	Scorodite	Okibe et al., 2014 [14]
20.0 (1500 ppm)	16.0	0.8		66	14	1.1	Scorodite	This study
	20.0	1.0	0.15	87		1.1	Scorodite	
	28.0	1.4		99		1.1	Scorodite	

4. Conclusions

- Morphological and structural characteristics of bio- and chemical- scorodite seed crystals were compared; bioscorodite ($\text{FeAsO}_4 \cdot 1.55\text{H}_2\text{O}$; spherical aggregates; 36 μm ; 2.0 m^2/g), chemical scorodite ($\text{FeAsO}_4 \cdot 1.91\text{H}_2\text{O}$; orthorhombic crystals; 98 μm ; 0.7 m^2/g). The former seeds showed greater stability (As; 0.33 ± 0.08 mg/L) than the latter (As; 5.49 ± 0.03 mg/L) by TCLP test.
- At pH 1.5, feeding bioscorodite seeds (0.15%) enabled effective As removal from dilute As(III) solution ($[\text{As(III)}]_{\text{ini}} = 4.7$ mM; $[\text{Fe(II)}]_{\text{ini}} = 9.5$ mM), by inducing a two-stage As and Fe precipitation (98% final As removal at day 21).
- Contrasting bioscorodite crystallization processes on bio- and chemical- scorodite seeds were found. Hollow bioscorodite seed particles became increasingly filled with newly formed scorodite, whilst solid chemical seeds induced their surface to be thoroughly coated with new scorodite precipitates.
- Lowering the initial pH from 1.5 to 1.2 (using bioscorodite seeds) led to a steady and continuous formation of bioscorodite particles (instead of two-stage As precipitation at pH 1.5). However, As removal remained relatively incomplete at pH 1.2 (91%) compared to at pH 1.5 (98%).
- TCLP leachabilities of final bioscorodite products formed on bio- and chemical- scorodite seeds (at pH 1.5) were 0.59 ± 0.08 mg/L and 1.86 ± 0.05 mg/L, respectively.
- Under the favorable conditions above described, 94–99% of As were successfully removed as crystalline bioscorodite from 3.3–20 mM As(III) solutions by setting initial $[\text{Fe(II)}]/[\text{As(III)}]$ molar ratios at 1.4–2.0.
- Optimal conditions found for the bioscorodite method enabling treatment of dilute As(III) concentrations did not necessarily match those found for chemical scorodite syntheses targeting high As(V) concentrations.
- For possible practical application using the continuous process (supposedly composed of an aeration tank followed by a settling tank), recycling microbiologically active bioscorodite sludge could maintain both high cell density and seed pulp density to support steady As(III) and Fe(II) oxidation and the resultant scorodite crystallization.

Acknowledgments: This work was partly supported by JSPS KAKENHI (Grant Numbers JP24760689 and JP15H02333) and Kurita Water and Environmental Foundation (KWEF Numbers 14A040 and 15K002). M.T. is grateful for financial assistance provided by the Kyushu University Advanced Graduate Program in Global Strategy for Green Asia.

Author Contributions: Masahito Tanaka performed the experiments and prepared the manuscript draft under the supervision of Naoko Okibe.

Conflicts of Interest: The authors declare no conflict of interest.

Appendix A

Table A1. Hydrolysis constants of Fe(III) and As(V) at 25 °C [19] and 70 °C calculated using the van't Hoff equation.

Ion Species	Hydrolysis Reaction	K_i	pK (25 °C) [19]	pK (70 °C)
Fe(III)	$\text{Fe}^{3+} + \text{H}_2\text{O} = \text{Fe(OH)}^{2+} + \text{H}^+$	K_{Fe1}	2.19	2.18
	$\text{Fe(OH)}^{2+} + \text{H}_2\text{O} = \text{Fe(OH)}_2^+ + \text{H}^+$	K_{Fe2}	3.48	3.47
	$\text{Fe(OH)}_2^+ + \text{H}_2\text{O} = \text{Fe(OH)}_3 + \text{H}^+$	K_{Fe3}	6.33	6.31
	$\text{Fe(OH)}_3 + \text{H}_2\text{O} = \text{Fe(OH)}_4^- + \text{H}^+$	K_{Fe4}	9.6	9.57
As(V)	$\text{H}_3\text{AsO}_4 = \text{H}_2\text{AsO}_4^- + \text{H}^+$	K_{As1}	2.24	2.27
	$\text{H}_2\text{AsO}_4^- = \text{HAsO}_4^{2-} + \text{H}^+$	K_{As2}	6.86	6.94
	$\text{HAsO}_4^{2-} = \text{AsO}_4^{3-} + \text{H}^+$	K_{As3}	11.49	11.51

Concentrations of Fe(III) and As(V) were determined as the activity of various dissolved ion species as shown in Equations (A1) and (A2).

$$\text{Fe(III)}_{\text{total}} = a_{\text{Fe}^{3+}} + a_{\text{Fe(OH)}^{2+}} + a_{\text{Fe(OH)}_2^+} + a_{\text{Fe(OH)}_3} + a_{\text{Fe(OH)}_4^-} \quad (\text{A1})$$

$$\text{As(V)}_{\text{total}} = a_{\text{AsO}_4^{3-}} + a_{\text{HAsO}_4^{2-}} + a_{\text{H}_2\text{AsO}_4^-} + a_{\text{H}_3\text{AsO}_4} \quad (\text{A2})$$

The equations for hydrolysis of Fe(III) (Equations (A3)–(A6)) and As(V) (Equations (A7)–(A9)) are based on the reactions shown in Table A1. Activities of Fe(III) and As(V) (Equations (3) and (4), respectively) are obtained by applying Equations (A3)–(A6) and (A7)–(A9) to Equations (A1) and (A2), respectively.

$$K_{\text{Fe1}} = \frac{[\text{Fe(OH)}^{2+}][\text{H}^+]}{[\text{Fe}^{3+}]} \quad (\text{A3})$$

$$K_{\text{Fe2}} = \frac{[\text{Fe(OH)}_2^+][\text{H}^+]}{[\text{Fe(OH)}^{2+}]} \quad (\text{A4})$$

$$K_{\text{Fe3}} = \frac{[\text{Fe(OH)}_3][\text{H}^+]}{[\text{Fe(OH)}_2^+]} \quad (\text{A5})$$

$$K_{\text{Fe4}} = \frac{[\text{Fe(OH)}_4^-][\text{H}^+]}{[\text{Fe(OH)}_3]} \quad (\text{A6})$$

$$K_{\text{As1}} = \frac{[\text{H}_2\text{AsO}_4^-][\text{H}^+]}{[\text{H}_3\text{AsO}_4]} \quad (\text{A7})$$

$$K_{\text{As2}} = \frac{[\text{HAsO}_4^{2-}][\text{H}^+]}{[\text{H}_2\text{AsO}_4^-]} \quad (\text{A8})$$

$$K_{\text{As3}} = \frac{[\text{AsO}_4^{3-}][\text{H}^+]}{[\text{HAsO}_4^{2-}]} \quad (\text{A9})$$

Table A2. Review of TCLP test results (revised from Gonzalez-Contreras et al., 2012 [12]).

Nature of Crystals	Size Crystals	Arsenic Leaching	
		TCLP Test (* pH 5, 20 h)	Arsenic Leaching at Other Test Conditions
Mineral			
Scorodite [29]	-	-	0.32 mg/L pH 2.43, 14 d (H ₂ SO ₄)
	-	-	1.49 mg/L pH 2.05, 14 d (H ₂ SO ₄)
Biogenic crystals			
Bioscorodite 72 °C [12]	Flakes < 1 cm	0.1 mg/L, 1 d 0.5 mg/L, 100 d	-
Bioscorodite 72 °C [13]	175 µm	1.9 mg/L, 60 d	-
Chemical synthesized crystals (70–95 °C)			
Nanocrystalline scorodite 70 °C [30]	50 nm	5.58 mg/L, 13 d	20.8 mg/L pH 1, 13 d
			0.56 mg/L pH 2, 13 d
			5.38 mg/L pH 7, 13 d
Amorphous ferric arsenate 70 °C [30]	50–100 nm	60 mg/L, 13 d	90 mg/L pH 2, 13 d
			30 mg/L pH 3, 13 d
			50 mg/L pH 4, 13 d
Scorodite 70 °C [31]	0.77 µm	5.13 mg/L, 7 h	2.69 mg/L pH 3.00, 7 h 1.01 mg/L pH 5.74, 7 h (water)
Scorodite 95 °C [16]	1.6 µm	13.6 mg/L, 18 h	-
	5.3 µm	0.1 mg/L, 18 h	-
Scorodite 95 °C [10]	16 µm	0.37 mg/L, 6 h	-
Scorodite 95 °C [17]	17 µm	0.18 mg/L, 35 d	0.4 mg/L pH 3, 35 d
			3.1 mg/L pH 7, 35 d
			351 mg/L pH 9, 35 d
Scorodite 95 °C [32]	-	0.3 mg/L, 4 h	0.45 mg/L pH 6, 4 h
Scorodite 95 °C [6] ^a	10 µm	4.8 mg/L*	-

Table A2. Cont.

Nature of Crystals	Size Crystals	Arsenic Leaching	
		TCLP Test (* pH 5, 20 h)	Arsenic Leaching at Other Test Conditions
Chemical synthesized crystals (150–175 °C)			
Scorodite 150 °C [16]	1.5 µm	13 mg/L, 8 h	-
	2.5 µm	5 mg/L, 8 h	
Scorodite 160 °C [33]	-	0.35 mg/L, 460 d	0.61 mg/L pH 6, 460 d 5.89 mg/L pH 7, 460 d
Scorodite 160 °C [34]	0.3 µm	0.35 mg/L, 460 d	5.89 mg/L pH 7, 460 d 386 mg/L pH 9, 460 d
Scorodite 160 °C [6] ^a	5 µm	0.8 mg/L *	-
Scorodite 160 °C [29]	2.5 µm	-	0.2 mg/L pH 5.57, 14 d (H ₂ SO ₄) 0.19 mg/L pH 3.45, 14 d (H ₂ SO ₄) 0.33 mg/L pH 2.85, 14 d (H ₂ SO ₄)
Scorodite 175 °C [35]	-	0.1 mg/L *	-

^a amended from the original Table by Gonzalez-Contreras et al., 2012 [12].

References

- Riveros, P.A.; Dutrizac, J.E.; Spencer, P. Arsenic disposal practices in the metallurgical industry. *Can. Metall. Quart.* **2001**, *40*, 395–420. [[CrossRef](#)]
- Dutrizac, J.E.; Jambor, J.L. The synthesis of crystalline scorodite, FeAsO₄·2H₂O. *Hydrometallurgy* **1988**, *19*, 377–384. [[CrossRef](#)]
- Monhemius, A.J.; Swash, P.M. Removing and stabilizing as from copper refining circuits by hydrothermal processing. *JOM* **1999**, *51*, 30–33. [[CrossRef](#)]
- Demopoulos, G.P.; Droppert, D.J.; Van Weert, G. Precipitation of crystalline scorodite (FeAsO₄·2H₂O) from chloride solutions. *Hydrometallurgy* **1995**, *38*, 245–261. [[CrossRef](#)]
- Filippou, D.; Demopoulos, G.P. Arsenic immobilization by controlled scorodite precipitation. *JOM* **1997**, *49*, 52–55. [[CrossRef](#)]
- Singhania, S.; Wang, Q.; Filippou, D.; Demopoulos, G.P. Temperature and seeding effects on the precipitation of scorodite from sulfate solutions under atmospheric-pressure conditions. *Metall. Mater. Trans. B* **2005**, *36*, 327–333. [[CrossRef](#)]
- Singhania, S.; Wang, Q.; Filippou, D.; Demopoulos, G.P. Acidity, valency and third-ion effects on the precipitation of scorodite from mixed sulfate solutions under atmospheric-pressure conditions. *Metall. Mater. Trans. B* **2006**, *37*, 189–197. [[CrossRef](#)]
- Fujita, T.; Taguchi, R.; Abumiya, M.; Matsumoto, M.; Shibata, E.; Nakamura, T. Novel atmospheric scorodite synthesis by oxidation of ferrous sulfate solution. Part I. *Hydrometallurgy* **2008**, *90*, 92–102. [[CrossRef](#)]
- Fujita, T.; Taguchi, R.; Abumiya, M.; Matsumoto, M.; Shibata, E.; Nakamura, T. Novel atmospheric scorodite synthesis by oxidation of ferrous sulfate solution. Part II. Effect of temperature and air. *Hydrometallurgy* **2008**, *90*, 85–91. [[CrossRef](#)]
- Fujita, T.; Taguchi, R.; Kubo, H.; Shibata, E.; Nakamura, T. Immobilization of arsenic from novel synthesized scorodite—Analysis on solubility and stability. *Mater. Trans.* **2009**, *50*, 321–331. [[CrossRef](#)]
- Gonzalez-Contreras, P.; Weijma, J.; van der Weijden, R.; Buisman, C.J.N. Biogenic scorodite crystallization by *Acidianus sulfidivorans* for arsenic removal. *Environ. Sci. Technol.* **2010**, *44*, 675–680. [[CrossRef](#)] [[PubMed](#)]
- Gonzalez-Contreras, P.; Weijma, J.; Buisman, C.J.N. Bioscorodite crystallization in an airlift reactor for arsenic removal. *Cryst. Growth Des.* **2012**, *12*, 2699–2706. [[CrossRef](#)]
- Gonzalez-Contreras, P.; Weijma, J.; Buisman, C.J.N. Continuous bioscorodite crystallization in CSTRs for arsenic removal and disposal. *Water Res.* **2012**, *46*, 5883–5892. [[CrossRef](#)] [[PubMed](#)]
- Okibe, N.; Koga, M.; Morishita, S.; Tanaka, M.; Heguri, S.; Asano, S.; Sasaki, K.; Hirajima, T. Microbial formation of crystalline scorodite for treatment of As(III)-bearing copper refinery process solution using *Acidianus brierleyi*. *Hydrometallurgy* **2014**, *143*, 34–41. [[CrossRef](#)]
- Okibe, N.; Morishita, S.; Tanaka, M.; Sasaki, K.; Hirajima, T.; Hatano, K.; Ohata, A. Bioscorodite crystallization using *Acidianus brierleyi*: Effects caused by Cu(II) present in As(III)-bearing copper refinery wastewaters. *Hydrometallurgy* **2017**, *168*, 121–126. [[CrossRef](#)]

16. Caetano, M.L.; Ciminelli, V.S.T.; Rocha, S.D.F.; Spitale, M.C.; Caldeira, C.L. Batch and continuous precipitation of scorodite from dilute industrial solutions. *Hydrometallurgy* **2009**, *95*, 44–52. [[CrossRef](#)]
17. Fujita, T.; Taguchi, R.; Abumiya, M.; Matsumoto, M.; Shibata, E.; Nakamura, T. Effect of pH on atmospheric scorodite synthesis by oxidation of ferrous ions: Physical properties and stability of the scorodite. *Hydrometallurgy* **2009**, *96*, 189–198. [[CrossRef](#)]
18. Johnson, D.B.; Joulain, C.; d’Hugues, P.; Hallberg, K.B. *Sulfobacillus benefaciens* sp. Nov., an acidophilic facultative anaerobic *Firmicute* isolated from mineral bioleaching operations. *Extremophiles* **2008**, *12*, 789–798. [[CrossRef](#)] [[PubMed](#)]
19. US EPA. *Method 1311: Toxicity Characteristic Leaching Procedure. Test Methods for Evaluating Solid Wastes Physical/Chemical Methods*; United States Environmental Protection Agency: Washington, DC, USA, 1992.
20. Dove, P.M.; Rimstidt, J.D. The solubility and stability of scorodite, $\text{FeAsO}_4 \cdot 2\text{H}_2\text{O}$. *Am. Mineral.* **1985**, *70*, 838–844.
21. Ondruš, P.; Skala, R.; Viti, C.; Veselovský, F.; Novák, F.; Jansa, J. Parascorodite, $\text{FeAsO}_4 \cdot 2\text{H}_2\text{O}$ —A new mineral from Kaňk near Kutná Hora, Czech Republic. *Am. Mineral.* **1999**, *84*, 1439–1444. [[CrossRef](#)]
22. Baghurst, D.R.; Barret, J.; Coleyshaw, E.E.; Griffith, W.P.; Mingos, D.M.P. Microwave techniques for the synthesis and deuteration of minerals, with particular reference to scorodite, $\text{FeAsO}_4 \cdot 2\text{H}_2\text{O}$. *Mineral. Mag.* **1996**, *60*, 821–828. [[CrossRef](#)]
23. Legal, J.M.; Manfait, M.; Theophanides, T. Applications of FTIR spectroscopy in structural studies of cells and bacteria. *J. Mol. Struct.* **1991**, *242*, 397–407. [[CrossRef](#)]
24. Langmuir, D.; Mahoney, J.; Rowson, J. Solubility products of amorphous ferric arsenate and crystalline scorodite ($\text{FeAsO}_4 \cdot 2\text{H}_2\text{O}$) and their application to arsenic behavior in buried mine tailings. *Geochim. Cosmochim. Acta* **2006**, *70*, 2942–2956. [[CrossRef](#)]
25. Gomez, M.A.; Becze, L.; Cutler, J.N.; Demopoulos, G.P. Hydrothermal reaction chemistry and characterization of ferric arsenate phases precipitated from $\text{Fe}_2(\text{SO}_4)_3\text{--As}_2\text{O}_5\text{--H}_2\text{SO}_4$ solutions. *Hydrometallurgy* **2011**, *107*, 74–90. [[CrossRef](#)]
26. Dutrizac, J.E.; Jambor, J.L. Characterization of the iron arsenate–sulphate compounds precipitated at elevated temperatures. *Hydrometallurgy* **2007**, *86*, 147–163. [[CrossRef](#)]
27. Gomez, M.A.; Becze, L.; Celikin, M.; Demopoulos, G.P. The effect of copper on the precipitation of scorodite ($\text{FeAsO}_4 \cdot 2\text{H}_2\text{O}$) under hydrothermal conditions: Evidence for a hydrated copper containing ferric arsenate sulfate–short lived intermediate. *J. Colloid Interface Sci.* **2011**, *360*, 508–518. [[CrossRef](#)] [[PubMed](#)]
28. Swash, P.M.; Monhemius, A.J. Hydrothermal precipitation from aqueous solutions containing iron(III), arsenate and sulphate. In *Hydrometallurgy '94*; Springer: Dordrecht, The Netherlands, 1994; pp. 177–190.
29. Krause, E.; Ettel, V.A. Solubility and stability of scorodite, $\text{FeAsO}_4 \cdot 2\text{H}_2\text{O}$: New data and further discussion. *Am. Mineral.* **1988**, *73*, 850–854.
30. Paktunc, D.; Bruggeman, K. Solubility of nanocrystalline scorodite and amorphous ferric arsenate: Implications for stabilization of arsenic in mine wastes. *Appl. Geochem.* **2010**, *25*, 674–683. [[CrossRef](#)]
31. Fujita, T.; Fujieda, S.; Shinoda, K.; Suzuki, S. Environmental leaching characteristics of scorodite synthesized with Fe(II) ions. *Hydrometallurgy* **2012**, *111*, 87–102. [[CrossRef](#)]
32. Harvey, M.C.; Schreiber, M.E.; Rimstidt, J.D.; Griffith, M.M. Scorodite dissolution kinetics: Implications for arsenic release. *Environ. Sci. Technol.* **2006**, *40*, 6709–6714. [[CrossRef](#)] [[PubMed](#)]
33. Bluteau, M.-C.; Demopoulos, G.P. The incongruent dissolution of scorodite—Solubility, kinetics and mechanism. *Hydrometallurgy* **2007**, *87*, 163–177. [[CrossRef](#)]
34. Bluteau, M.-C.; Becze, L.; Demopoulos, G.P. The dissolution of scorodite in gypsum-saturated waters: Evidence of Ca-Fe-AsO_4 mineral formation and its impact on arsenic retention. *Hydrometallurgy* **2009**, *97*, 221–227. [[CrossRef](#)]
35. Gomez, M.; Becze, L.; Bluteau, M.; Le Berre, J.; Cutler, J.; Demopoulos, G. Autoclave precipitation and characterization of Fe(III)– $\text{AsO}_4\text{--SO}_4$ phases. *Hydrometallurgy* **2008**, *8*, 1078–1085.

